Anal Bioanal Chem
DOI 10.1007/s00216-014-8074-3

RESEARCH PAPER

Applicability of UV laser-induced solid-state fluorescence spectroscopy for characterization of solid dosage forms

Eva Woltmann · Hans Meyer · Diana Weigel · Heinz Pritzke · Tjorben N. Posch · Pablo A. Kler · Klaus Schürmann · Jörg Roscher · Carolin Huhn

Received: 17 March 2014 / Revised: 23 July 2014 / Accepted: 28 July 2014

Abstract High production output of solid pharmaceutical formulations requires fast methods to ensure their quality. Likewise, fast analytical procedures are required in forensic sciences, for example at customs, to substantiate an initial suspicion. We here present the design and the optimization of an instrumental setup for rapid and non-invasive characterization of tablets by laser-induced fluorescence spectroscopy (with a UV-laser (λ_{ex}=266 nm) as excitation source) in reflection geometry. The setup was first validated with regard to repeatability, bleaching phenomena, and sensitivity. The effect on the spectra by the physical and chemical properties of the samples, e.g. their hardness, homogeneity, chemical composition, and granule grain size of the uncompressed material, using a series of tablets, manufactured in accordance with design of experiments, was investigated. Investigation of tablets with regard to homogeneity, especially, is extremely important in pharmaceutical production processes. We demonstrate that multiplicative scatter correction is an appropriate tool for data preprocessing of fluorescence spectra. Tablets with different physical and chemical characteristics can be discriminated well from their fluorescence spectra by subjecting the results to principal component analysis.

Keywords Tablet analysis · Solid-state fluorescence spectroscopy · Grain size · Photobleaching · Scattering effects · Homogeneity

E. Woltmann · T. N. Posch · P. A. Kler · C. Huhn
Central Institute for Engineering, Electronics and Analytics: Analytics (ZEA-3), Forschungszentrum Jülich, 52428 Jülich, Germany

H. Meyer
J&M Analytik AG, 73457 Essingen, Germany

D. Weigel
Federal Criminal Police Office, Forensic Science Institute, KT 34 – Toxicology, 65193 Wiesbaden, Germany

H. Pritzke
Glatt Systemtechnik GmbH, 01277 Dresden, Germany

P. A. Kler · C. Huhn (✉)
Institute of Physical and Theoretical Chemistry, Eberhard Karls Universität Tübingen, 72076 Tübingen, Germany
e-mail: carolin.huhn@uni-tuebingen.de

K. Schürmann
LabCognition Analytical Software GmbH & Co. KG, 50825 Köln, Germany

J. Roscher
Institute of Inorganic and Analytical Chemistry, Westfälische Wilhelms-Universität Münster, 48149 Münster, Germany

Introduction

Tablets and other solid dosage forms are the most common pharmaceuticals [1–3], because they are convenient for the patient to handle [1] but also because of greater drug stability compared with liquid dosage forms [4]. Moreover, individual design of a tablet helps to increase the bioavailability of the active agent according to therapeutic requirements, and thus helps to increase the effectiveness of the drug [5].

High demands on quality control in industry and high production output increase the need for reliable and rapid methods for analysis of solids. Non-destructive techniques based on optical spectroscopy usually require neither sample preparation nor long analysis time and are, consequently, preferred to time-consuming analysis based on chromatography or capillary electrophoresis for high throughput analysis. Although classical approaches provide detailed information on the chemical composition of a sample, they fail to provide information on its physical characteristics. Because NIR, Raman, and fluorescence spectra are affected by the microenvironment of the analyte, they also provide information on the

Published online: 09 August 2014

sample's physical properties. A variety of methods for investigation of pharmaceutical solids by use of NIR spectroscopy have been described in the literature [1]. In the forensic sciences, NIR and Raman spectroscopy are used for identification of counterfeit drugs [6–8]. Here, physical, chemical, and physicochemical properties, for example the concentration and type of the active agent (side products) [9], the tableting material, the form of the active pharmaceutical ingredient (API), and overall quality with regard to homogeneity, shape, colorants, and compaction, are important properties for discrimination of counterfeit products from the original.

Compared with NIR or Raman spectroscopy, solid-state fluorescence spectroscopy has rarely been used for quality control in industry or in the forensic sciences, although it can be assumed to be highly applicable, because many active agents are native fluorophores, as a result of their large conjugated π-electron systems. Fluorescence spectroscopy has the additional advantage of high sensitivity. It is known that fluorescence spectra are affected by conformational changes of the fluorophore, intermolecular interactions between fluorophores, and interactions between the fluorophore and other components of the sample but these effects are not well understood and further basic research is required for this method to become accepted [10].

In contrast with analysis of pharmaceutical solids, fluorescence analysis is often applied in solution, especially in combination with HPLC and CE. Fluorescence methods enable detection down to concentrations of 10^{-10} mol L^{-1} or even lower [11]. Detection of active agents in solution has been reported by Navalon et al. [12], who measured acetylsalicylic acid (ASA) calibration standards down to a concentration of 2.00 μg mL^{-1}.

The few studies described in literature on the use of fluorescence spectroscopy for analysis of tablets and/or solid pharmaceutical dosage forms have shown that this method has advantages similar to those of Raman or NIR spectroscopy in terms of simplicity and rapidity: Moreira et al. [13] worked with a xenon discharge lamp as an excitation source to detect ASA in excipients. They described a non-destructive technique which does not require sample preparation. Use of a xenon discharge lamp rather than a laser, such as that used for our experiments described below, has the advantage of individual wavelength optimization for each sample and/or analyte. However, intensities are usually poor at low UV wavelengths. In this study, we use a frequency quadrupled Nd:YAG UV-laser emitting light at λ_{ex}=266 nm; this has the advantage of being a well focusable light source of high intensity, suitable for efficient excitation of even small amounts of active agent, impurities, or weak native fluorophores.

Optical spectra contain chemical information, e.g. about the sample's composition and such physical properties as compaction, grain size, and shape. Both positive and, more often, negative aspects related to interferences caused by the physical characteristics of the sample are reported in the literature [14, 15]. These interferences can be used for discrimination of tablets manufactured with different physical properties, e.g. hardness. If information on the chemical composition of the sample is required, results must be preprocessed by use of such mathematical tools as multiplicative scatter correction (MSC), extended multiplicative scatter correction (EMSC), or standard normal variate (SNV), to remove interferences in spectra related to the physical properties of the sample which often obscure information about the sample's composition. These preprocessing tools are widely used in NIR and Raman spectroscopy [6, 16, 17].

In this paper we report the development of a new and straightforward method for characterization of pharmaceutical solids and for identification of counterfeit medicine on the basis of laser-induced fluorescence spectroscopy (LIF). The setup is characterized with regard to its sensitivity, robustness, and geometry by using fluorescent TLC plates and commercial ASA tablets as model samples. The broadness of its applicability is demonstrated for several commercial tablets containing different types of active agent. Because a very powerful excitation source is used to induce fluorescence, we also studied bleaching effects of the model substances. In the second part of the study, we investigated the suitability of the system for characterization of the chemical and physical properties for a series of tablets that was designed especially for this study in accordance with design of experiments (DoE).

Materials and methods

Setup

The setup used for LIF measurements of tablets is shown in Fig. 1A. A frequency quadrupled Nd:YAG laser (FQSS 266-Q2, 266 nm, quasi-cw power approx. 10 mW; CryLaS, Berlin, Germany) was used as excitation source. The laser beam is guided through the inner part of a y-optical fiber (J&M Analytik AG, Essingen, Germany) to the sample, where fluorescence is induced. Scattered and emitted light enters a set of 12 optical fibers surrounding the core excitation fiber. A filter system (two edge filters: HR 266 nm, HT>310 nm, >6 OD; J&M Analytik AG) was placed between sample and detector to prevent scattered light from the laser beam reaching the CCD camera used as detector (Tidas CCD UV/NIR; J&M Analytik AG). The distance between the sample holder and the end of the fiber is variable via the lengths h and k (Fig. 1A, B). Via h_{set}, the distance between the end of the fiber and the sample holder can be changed in a wide range; the minimum distance is 1.4 cm. The actual distance between the end of the optical fiber and the sample can easily be calculated from the set distance between the fiber and the sample holder, h_{set}, and

the thickness of the tablet, d_t: $h=h_{set}-d_t$. Fine tuning of the absolute distance between the end of the fiber and the sample is possible by adjustment of the length k.

An LED (LEDMOD 365.100, λ_{ex}=360–370 nm, $P_0\leq$ 500 mW; Omicron Laserage, Rodgau, Germany) was used to demonstrate the versatility of the setup with regard to exchange of the light source.

The settings were:

- measurements described in the sections "Applicability", "Bleaching phenomena", "Effect on detected fluorescence intensity of the distance between the end of the optical fiber and the sample", "Repeatability", and "Flexibility of the setup": 1 s (10 replicate measurements were averaged);
- measurements described in the section "Sensitivity and linearity": integration time 100 ms (three replicate measurements were averaged); and
- measurements described in the section "Discrimination of tablets with different chemical and physical properties": integration time 1 s (10 replicate measurements were averaged); 8–10 tablets of each type were analyzed (Table 3)

A dark spectrum was subtracted from every individual spectrum. Measurements were performed by use of Panorama software (LabCognition Analytical Software, Cologne, Germany). IGOR Pro (Wavemetrics, Lake Oswego, Oregon, USA) and Unscrambler (Camo Software, Oslo, Norway) were used for data evaluation. Mean centered data were subjected to principal component analysis (PCA) by use of the NIPALS algorithm (leverage correction).

Samples

All measurements were performed without further sample preparation. Commercially available products were: fluorescent TLC plates (silica gel, 60, F254; Merck, Darmstadt, Germany), ASS+C effervescent tablets (600 mg acetylsalicylic acid; Ratiopharm, Ulm, Germany), tamoxifen tablets (40 mg; Hexal, Holzkirchen, Germany), Tramadol AL 50 effervescent tablets (AL Pharma, Laichingen, Germany), brewer's yeast tablets (Haiterbach, Haiterbach, Germany), ASS tablets (500 mg; AL Pharma), and ASS tablets (500 mg; Stada, Bad Vilbel, Germany).

For in-house fabrication of the tablets, the following chemicals (provided by Glatt Systemtechnik, Dresden, Germany) were used: *o*-acetylsalicylic acid (ASA; 99 %; Alfa Aesar, Karlsruhe, Germany); Aerosil 200 (Overlack, Mönchengladbach, Germany); caffeine (Fagron, Barsbüttel, Germany); chloroquine, diphosphate salt (Alfa Aesar); erythrosine (Colorcon, Harleysville, PA, USA); Kollidon VA 64 (BASF, Ludwigshafen, Germany); lactose monohydrate (DMV–Fonterra Excipients, Goch, Germany); Ludipress (BASF); magnesium stearate (AppliChem, Darmstadt, Germany); quinine sulfate dihydrate (Azelis Deutschland Pharma, Krefeld, Germany); starch (1500 partially pregelatinized maize starch; Coloron, Dartford, Kent, UK); talcum (technical; VWR, Darmstadt, Germany).

For calibration with *o*-acetylsalicylic acid, chloroquine diphosphate, and quinine sulfate dihydrate a series of tablets with different content of each compound was prepared by use of an eccentric press (EK0; Korsch, Berlin, Germany). A stock mixture containing Kollidon VA 64 (24.4 %), magnesium stearate (2.4 %), Aerosil (2.4 %), maize starch (48.8 %), and talcum (22.0 %) was sieved and mixed. Final ratios of active agent to lactose monohydrate to stock mixture are summarized in Table 1. After further manual mixing, tablets were compressed.

Tablets for the DoE (composition given in Table 2) were manufactured in accordance with the design given in Table 3 (by Glatt Systemtechnik using a Fette Compacting 102i press from Glatt Ingenieurtechnik, Weimar, Germany) including samples with different composition, hardness (compression force between 5.7 and 19.6 kN), granule grain size (varied by changing the granulation time and the amount of liquid added during the granulation process), tableting technique (directly or including previous granulation), and homogeneity (for Series m (Table 2) the API was folded manually into the matrix). Tablets were stored in blister packages. The thickness (d_t) varied for tablets of different hardness by less than 1 mm (d_t=0.43–0.52 cm) which can be neglected for our analysis.

For demonstration of the flexibility of the setup regarding optimization of the wavelength, two series of tablets (provided by Glatt Systemtechnik) containing the same amount of API (formulation M1), one containing a red colorant (erythrosine) and one without any colorant were used.

Results and discussion

Method optimization and validation

Applicability

Measurements were performed in reflectance geometry (at 90 degrees to the surface of the (flat) sample), because this is easiest to handle, especially for samples with a large curvature. To demonstrate the suitability of the setup, measurements (integration time 1 s, 10 replicate measurements were averaged) were performed with an ASA tablet (AL Pharma), a brewer's yeast tablet, a tamoxifen tablet, and a tramadol tablet (Fig. 2, distance$h$ optimized for each sample in accordance with intensity: h=2.71 cm for the ASA tablet (d_t=0.44 cm) (A), h=0.87 cm for the Brewer's yeast tablet (d_t=0.53 cm)

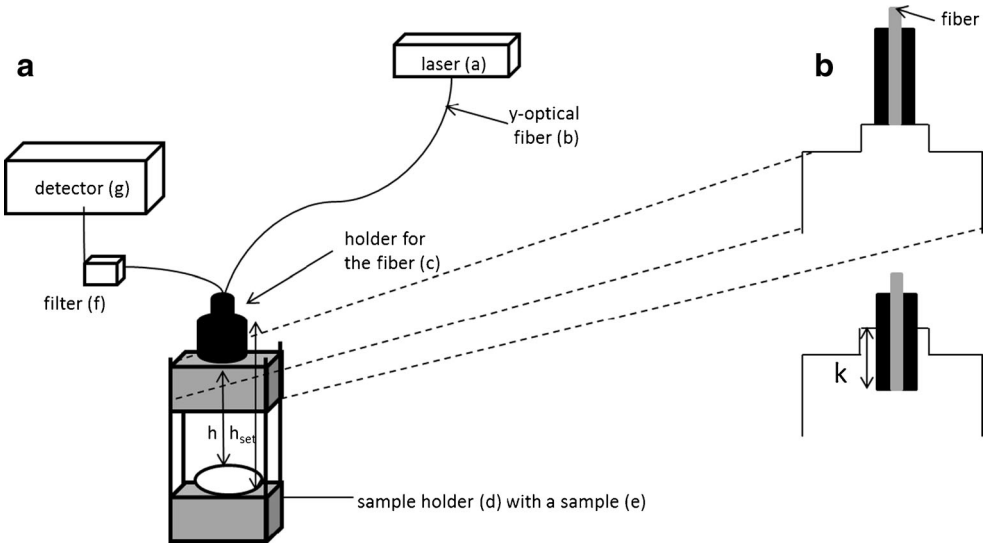

Fig. 1 (**A**) Schematic diagram of the setup: (*a*) laser (Nd:YAG, λ_{ex}=266 nm, 10 mW), (*b*) y-optical fiber, (*c*) holder for the fiber, (*d*) sample holder with adjustable z-axis, (*e*) sample, (*f*) filter system, (*g*) detector (CCD camera); (**B**) enlarged view of the fiber holder with fine tuning via length *k*

(B), h=0.9 cm for the tamoxifen tablet (d_t=0.5 cm) (C), and h=1.04 cm for the tramadol tablet (d_t=0.36 cm) (D); fine tuning via k was not accomplished in this pre-study (k=0)).

Each spectrum has a different characteristic pattern, enabling rapid discrimination of the tablets. Fluorescence spectra of the ASA tablet and the brewer's yeast tablet have an intensity maximum at approximately 450 nm. Fluorescence spectra of tamoxifen and tramadol have more complex profiles at low wavelengths (Fig. 2). Although measurement with the ASA tablet was conducted with the largest distance h between the end of the optical fiber and the sample, this signal was twice as intense as the maximum fluorescence intensity measured for the tramadol tablet. This is presumably caused by a higher fluorescence quantum yield and the high concentration of ASA (c_{ASA}=78 %, $c_{tramadol}$=4 %; quantitative aspects are discussed in the section "Sensitivity and linearity"). There is a second sharp band with a maximum at λ_{em}=805 nm in every spectrum; this can be assigned to the emission wavelength of the laser's pump laser diode. This signal is solely affected by scattering effects on the surface of the sample.

Bleaching phenomena

Photobleaching is well known in fluorescence spectroscopy especially when using bright excitation sources. The mechanism was discussed in detail by Song et al. [18] for fluorescein. Accordingly, photobleaching on an ASS+C effervescent tablet and a TLC plate was investigated by irradiating a small spot for 10 s (integration time 1 s, 10 replicate measurements were averaged) 10 times (total 100 s)) while recording the fluorescence spectra. Figure 3 shows the maximum intensity of each spectrum ($\lambda_{max,ASS}$=421.8±1.5 nm, $\lambda_{max,TLC}$=527.5 ±0 nm; h=3.15 cm for the TLC plate and h=2.67 cm for the ASS+C tablet).

For the TLC plate and the ASS tablet, the maximum intensity decreased exponentially (fit data listed in Fig. 3) with irradiation time, in accordance with the kinetics described by Song et al. [18]. Decay of the detected fluorescence intensity was faster for the measurements with the ASS tablet (K_3= 0.0243) compared with measurements with the TLC plates (K_3=0.0035). The uncertainty of the measurements caused by

Table 1 Relative proportions of the API (=ASA, quinine sulfate dihydrate or chloroquine diphosphate), stock mixture (containing Kollidon VA 64 (24.4 %), magnesium stearate (2.4 %), Aerosil (2.4 %), maize starch (48.8 %), talcum (22.0 %)), and lactose monohydrate in the tablets (diameter of the tablets d_{tablet}=11.15 mm)

API/%	stock mixture/%	lactose monohydrate/%
25	20.5	54.5
10	20.5	69.5
5	20.5	74.5
1	20.5	78.5
0.1	20.5	79.4
0.01	20.5	79.49

Table 2 Composition of the tablets manufactured by Glatt Systemtechnik

Mixture 1 [M1] (substance: % (*w*/*w*))	Mixture 2 [M2] (substance: % (*w*/*w*))
Quinine sulfate (dihydrate): 1	Quinine sulfate (dihydrate): 4
Caffeine: 10	Caffeine: 7
Lactose monohydrate: 68.5	Lactose monohydrate: 68.5
Kollidon VA 64: 5	Kollidon VA 64: 5
Magnesium stearate: 0.5	Magnesium stearate: 0.5
Aerosil: 0.5	Aerosil: 0.5
Maize starch: 10	Maize starch: 10
Talcum: 4.5	Talcum: 4.5

Table 3 Production details for the samples

Sample name[a]	Composition	Compression force (kN)	Tableting technique[b]	Grain size[c]
L1	M1	19.6	◊	P
L2	M1	13.8–14.0	◊	P
L3	M1	8.5–8.6	◊	P
L4	M1	5.7–5.8	◊	P
K1	M1	19.6	◊	Q
K2	M1	13.8–14.0	◊	Q
K3	M1	8.5–8.6	◊	Q
K4	M1	5.7–5.8	◊	Q
m1	M1	19.6	▫	
m2	M1	13.8–14.0	▫	
m3	M1	8.5–8.6	▫	
m4	M1	5.7–5.8	▫	
N1	M2	19.6	▫	
N2	M2	13.8–14.0	▫	
N3	M2	8.5–8.6	▫	
N4	M2	5.7–5.8	▫	

[a] Upper case letters, homogeneous samples; lower case letters, inhomogeneous samples

[b] ▫, direct compression; ◊, compression after granulation

[c] P, average grain size=286.8 μm; Q, average grain size=674.0 μm

counting statistics can be neglected. The results clearly show that the chemical composition of the irradiated sample spot changes, thus the method is not fully non-destructive, in contrast with other methods reported in literature based on induced fluorescence, e.g. analysis of stone substrates [19]. The destructiveness of the method can partially be counteracted by choosing suitable integration times for the measurements: increasing the integration and/or irradiation time for measurements with samples containing a photolabile active agent at low concentration does not necessarily lead to a substantial increase of the fluorescence intensity, because the analyte might decompose. Care must be taken if experiments have to be repeated, or if the sample has to be reanalyzed by another method, e.g. to reinforce an initial counterfeit suspicion at customs.

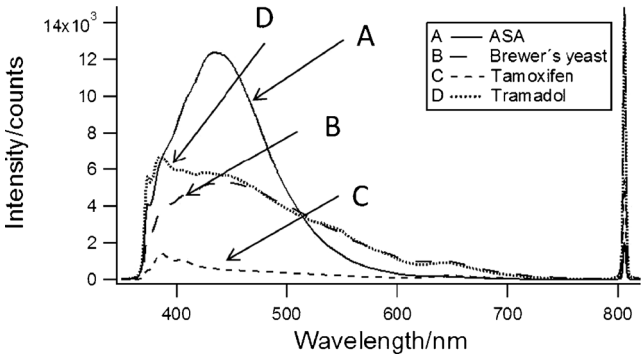

Fig. 2 Fluorescence spectra of: ASA tablet (*A*), *h*=2.71 cm; brewer's yeast (*B*), *h*=0.87 cm; tamoxifen tablet (*C*), *h*=0.9 cm; tramadol tablet (*D*), *h*=1.04 cm; λ_{ex}=266 nm; integration time 1 s (10 replicate measurements were averaged)

Effect on detected fluorescence intensity of the distance between the end of the optical fiber and the sample

The irradiated area of the sample, the intensity of the excitation beam area reaching the sample, and the fluorescence light collection efficiency depends on the distance between the end of the optical fiber and the sample. This was investigated by using large (>>laser spot) fluorescent TLC plates (*h*= 3.15 cm, 3.95 cm, 4.45 cm) and ASS+C effervescent tablets (*h*=2.67 cm, 3.47 cm, 3.97 cm; d_t=0.48 cm, diameter of the ASA tablet d_{ASA}=2.52 cm) as model samples and varying the distance*h*. Measurements with the effervescent tablet were performed with the laser spot centered on the tablet to ensure high repeatability. As shown in Fig. 4, the intensity of the fluorescence signal decreases with increasing distance*h* for both samples. Three processes must be taken into account to explain this result.

1. The decrease of the intensity per area of the excitation beam reaching the sample with increasing*h*. This is negligible because of the high intensity of the excitation beam.
2. The area irradiated by the laser beam and the size of the tablets. It is important to note that even the largest diameter of the irradiated sample area of 1.8 cm (for *h*= 3.97 cm) is smaller than the diameter of the sample itself (d_{ASA}=2.52 cm). Using the numerical aperture (*NA*= 0.22) and the diameter of the optical fiber (*d*=600 μm), the spot size diameter on the sample was calculated for different distances*h* (refractive index of ambient air n_i=1; Fig. 4, right axis). As expected, spot size diameter increases linearly with increasing distance*h*.

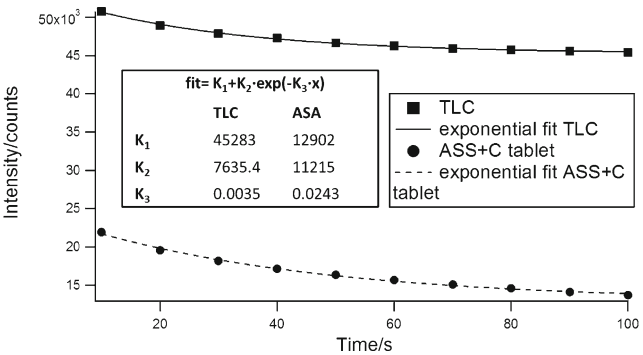

Fig. 3 Investigation of the effect of photobleaching of the sample caused by laser radiation (λ_{ex}=266 nm; *h*=3.15 cm for the TLC plate; *h*= 2.67 cm for the ASS+C tablet, d_t=0.48 cm; $\lambda_{max,ASS}$=421.8±1.5 nm, $\lambda_{max,TLC}$=528.6±0 nm); integration time 1 s (10 replicate measurements were averaged)

3. For small distances *h*, detection of the fluorescence light is possible over a larger dihedral angle. Because the detected fluorescence intensity decreases with increasing distance between the optical fiber and the sample (Fig. 4), detection over a smaller dihedral angle seems to have a stronger effect on the intensity than the size of the area irradiated.

This is important information for improvement of the detection system: on the one hand, very strong fluorophores at high concentration must be analyzed at a larger distance *h* to avoid overloading. On the other hand, for a fluorophore present at low concentration only or with a low fluorescent quantum yield, reducing the distance *h* improves detection. Another option is to reduce or increase the integration time to adapt to the intensity of the recorded signal. The setup is therefore flexible for samples with a fluorophore as the main compound but also for fluorescent trace contamination.

The size of the sampled area is especially important for investigation of inhomogeneous samples. For small distances *h*, only a small area is probed and thus sub-sampling might occur, in contrast with probing a larger area at a larger distance *h*; this has also been discussed for Raman spectroscopy (wide area illumination) [1, 20].

Repeatability

Fluorescent TLC plates were chosen as model samples with a flat surface and a homogeneously distributed fluorophore to investigate the repeatability of measurements performed with the setup presented (Fig. 1). The laser output was proved to be stable (*RSD*=0.62 % for intensity over 3 min, detected with a with a photomultiplier tube). To avoid the effects of bleaching phenomena, measurements (integration time 1 s, 10 replicate measurements were averaged) were conducted at different non-overlapping spots on the plate (*h*=3.95 cm, spot size area 2.66 cm^2 (*d*=1.84 cm)). The RSD value of the maximum intensity was calculated to be 1.0 % (*n*=10) demonstrating repeatability was high.

Sensitivity and linearity

Calibration was performed for the three model substances (ASA, quinine sulfate dihydrate, and chloroquine diphosphate) with a series of manually prepared tablets for each fluorophore (d_{tablet}=11.15 mm) containing 0 (blanks), 0.01, 0.1, 1, 5, 10, or 25 % (*w*/*w*) of the analyte. All measurements were performed at the center of the tablet, to ensure high repeatability, at three different distances between the optical fiber and the sample (*h*=2.5 cm, 5.0 cm, 6.3 cm, d_t=0.22 cm, integration time 100 ms, three replicate measurements were averaged; number of replicates for each concentration: *n*=2).

The maximum intensity of the fluorescence bands of ASA tablets and chloroquine tablets was determined, and the

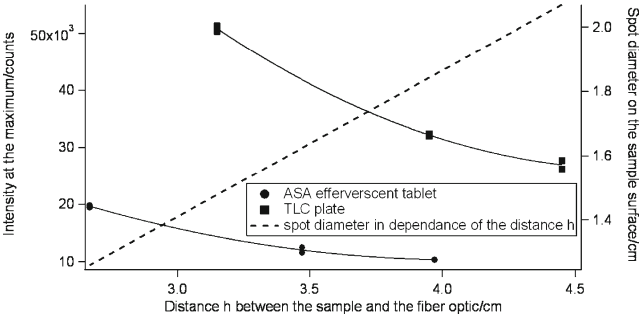

Fig. 4 Dependence of fluorescence intensity and spot size diameter on the distance *h* between the end of the fiber and the sample (TLC plate: *h*= 3.2 cm, 4.0 cm, 4.5 cm; ASS+C effervescent tablet (d_t=0.48 cm): *h*= 2.7 cm, 3.5 cm, 4.0 cm; λ_{ex}=266 nm, integration time 1 s (10 replicate measurements were averaged), two measurements for each distance)

calibration curves were established (Fig. 5a, chloroquine diphosphate; Fig. 5b, *o*-acetylsalicylic acid; averaged values of two measurements). In addition, the fluorescence intensity of a commercial ASA tablet was added for comparison (Stada, Fig. 5b, marked with *). The intensity at λ_{em}=450 nm (maximum intensity was not reliable) in the spectra obtained from tablets with different quinine sulfate content was used to establish a calibration curve for quinine sulfate dihydrate (Fig. 5c). The fluorescence spectra of tablets containing 1 % (*w*/*w*) fluorophore (*h*=2.5 cm) are shown. Of course the quality, especially the homogeneity, of the manually mixed tablets is inferior to that of commercially manufactured tablets.

The overall trend of the calibration curves for *o*-acetylsalicylic acid, chloroquine diphosphate, and quinine sulfate does not change for different distances *h* between the sample and the end of the optical fiber; measured intensities are, however, higher for small distances *h*.

Quantitative analysis was possible down to a concentration of 1 % (*w*/*w*) for quinine sulfate dihydrate for all distances, because these tablets can clearly be distinguished from the tablets composed of tableting material only (*h*=2.5 cm: $I_{450\ nm,blank}$= *107.3,* $I_{450\ nm,1}$=432.2; *h*=5.0 cm: $I_{450\ nm,blank}$= 25.2, $I_{450\ nm,1}$=111.0, *h*=6.3 cm: $I_{450\ nm,blank}$=9.2, $I_{450\ nm,1}$= 38.3) and 1 % (*w*/*w*) for chloroquine diphosphate (*h*=2.5 cm: $I_{max,blank}$=120.3, $I_{max,1}$=213.3; *h*=5.0 cm: $I_{max,blank}$=28.0, $I_{max,1}$= *52.7,* *h*=6.3 cm: $I_{max,blank}$=10.5, $I_{max,1}$=18.2). The detection capability for ASA is as low as 0.01 % (*w*/*w*) for all distances (*h*=2.5 cm: $I_{max,blank}$=120.3, $I_{max,0.01}$=301.0; *h*= 5.0 cm: $I_{max,blank}$=28.0, $I_{max,0.01}$=75.5, *h*=6.3 cm: $I_{max,blank}$= *11.2,* $I_{max,0.01}$=28.3). These results are comparable with those from other studies. For example, Moreira et al. [13] reported limits of detection and quantification of 0.22 and 0.73 % (*w*/*w*) for ASA in powdered matrix material (not compressed) with a xenon discharge lamp (20 kW, 8 μs pulse duration, wavelength not given). The detection capability for ASA with our setup is estimated to be approximately 20 times better. The low detection limits for the substances are

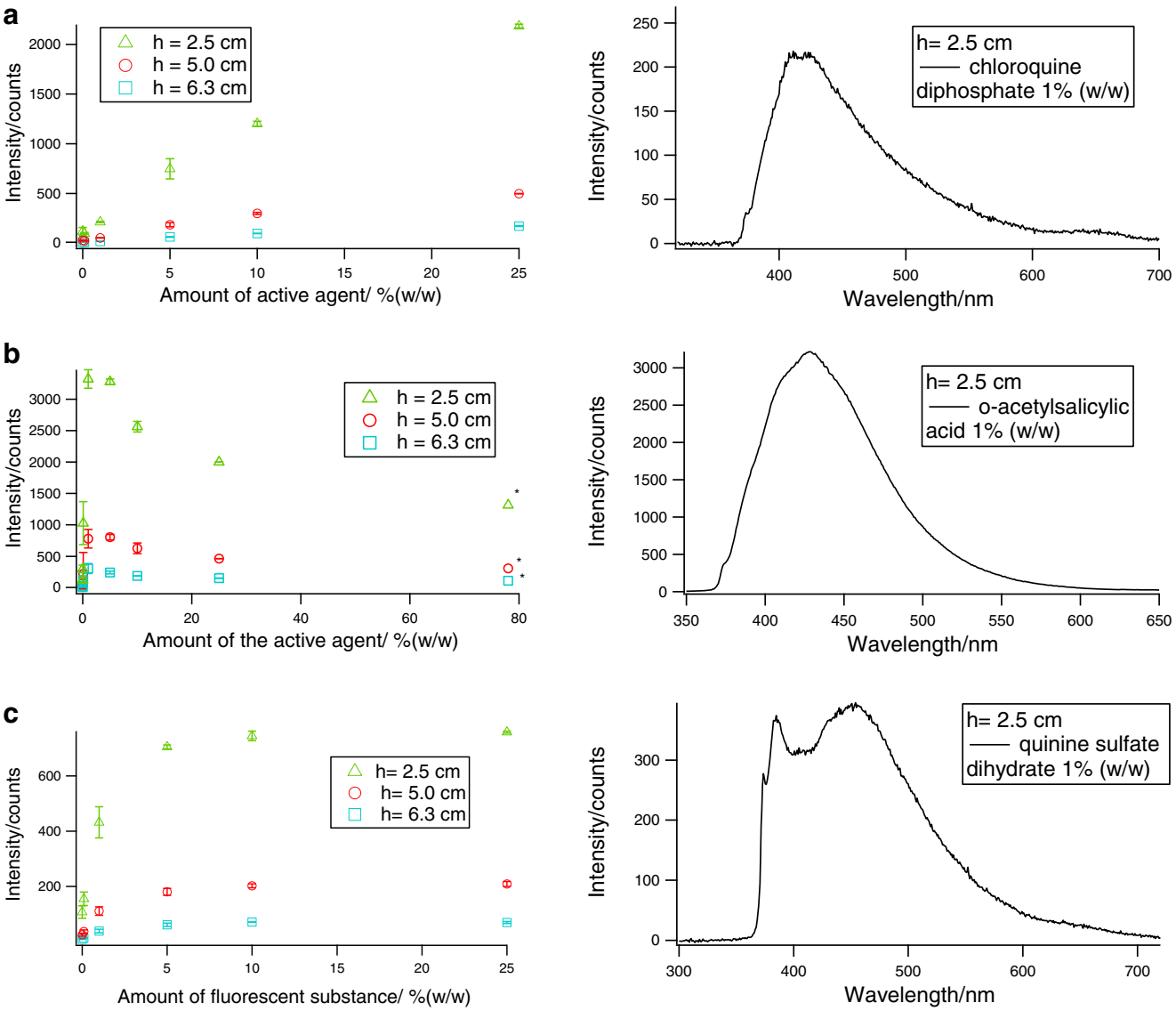

Fig. 5 Calibration curve (*left*) for tablets containing chloroquine diphosphate (**a**), *o*-acetylsalicylic acid (**b**), and quinine sulfate dihydrate (**c**), h= 2.5 cm, 5.0 cm, 6.3 cm; and the fluorescence spectra (h=2.5 cm, 1 % (*w*/*w*)) of these substances (*right*), d_t=0.22 cm; λ_{ex}=266 nm, integration time 100 ms (three replicate measurements were averaged), number of replicates for each concentration: n=2; *asterisk*, commercial ASA tablet

indicative of potential applicability of the method in pharmaceutical industry, e.g. for detection of fluorescent trace contamination. The limit of detection can even be improved by reducing the distance, h, between the sample and the end of the optical fiber (as discussed in the section "Effect on detected fluorescence intensity of the distance between the end of the optical fiber and the sample"). To analyze solid pharmaceuticals containing two fluorescent components (active agent and reactant as an impurity or two active agents), Villari et al. [21] worked with a 200-W xenon–mercury excitation source for investigation of salicylic acid impurities in acetylsalicylic acid. The method enables investigation of salicylic acid impurities in acetylsalicylic acid in the range 0.01–2 % (*w*/*w*).

The fluorescence intensity increases linearly with increasing amount of chloroquine diphosphate within the concentration range investigated (0 and 25 % (*w*/*w*)). For tablets containing quinine sulfate dihydrate (Fig. 5a) within the concentration range 0–5 % (*w*/*w*), the intensity also increases linearly with increasing amount of the analyte. In these concentration ranges quantification of the fluorophore is possible. For higher concentrations of quinine sulfate dihydrate, the slope of the plot of fluorescence intensity against concentration decreases, as already described for other substances by Head [22]. He explained this effect as self-quenching, similar to effects at high concentration in solution.

The pattern of the calibration curve for ASA is different. Up to a concentration of 1 % (*w*/*w*), the intensity of the

detected fluorescence increases almost linearly with increasing amount of active agent, reaches a plateau in the range between 1 and 10 % (*w*/*w*), but then decreases almost linearly for concentrations >10 % (*w*/*w*) (Fig. 5b). The ASA content of a tablet can be determined with our method for low or high fluorophore content, because the intensity of the signal increases or decreases linearly in the concentration ranges between 0.01 and 1 % (*w*/*w*) and between 10 and 78 % (*w*/*w*), respectively, though prior knowledge of the expected concentration range is required. The relationship between fluorescence intensity and API content can be explained by two effects.

1. Because of self-quenching effects, a decrease of the slope of a plot of intensity vs. concentration can be expected at high concentration. Head [22] investigated the fluorescence properties of sodium salicylate at different concentrations using 310 nm as the excitation wavelength and detecting fluorescence at 415 nm. Samples containing 0, 25, 50, 75, and 100 % of the fluorophore were investigated. The decreasing slope of the calibration curve was explained by Head [22] on the basis of self-quenching effects.
2. For the second explanation, the absorption properties of the fluorophore must be taken into account. The Stokes shift for ASA is small [13, 23] and thus re-absorption of emitted light by the sample might occur, causing a decrease of fluorescence intensity, especially at high concentrations. This is a well-known problem limiting the analysis of many organic compounds [24]. Re-absorption phenomena do not affect measurements carried out with substances with a large Stokes shift, for example quinine sulfate, with an absorbance maximum at approximately 250 nm (at higher wavelengths (350–400 nm) the absorbance is of low intensity only) and a fluorescence maximum >370 nm [25].

Physical properties of the samples, for example roughness and macroscopic structure, affect the signal intensity of spectra, as discussed by Head [22] for fluorescence spectroscopy. Merckle et al. [26] observed an effect on NIR spectra caused by a different hardness of the tablet and thus different structures of the surface of the tablet. Figure 5b shows the calibration curve of ASA measured with manually prepared tablets in the concentration range between 0 and 25 % (*w*/*w*). Measurement of a commercial ASA-tablet was also conducted; the maximum fluorescence intensity of this measurement is also plotted in Fig. 5b. Different physical properties of commercial and manually prepared tablets can be assumed. The value of the fluorescence intensity measured for the commercial ASA tablet fits the pattern of the calibration curve measured with the manually prepared tablets (linear decrease in concentration range between 10 and 25 % (*w*/*w*)). The effect of the matrix material can obviously be neglected at higher ASA concentrations.

Flexibility of the setup

The use of fiber optics enables rapid and simple exchange of the light sources. This flexibility enables wavelength optimization for different analytes. Fluorescence measurements were performed with different excitation wavelengths for two tablets with the same composition except that one was colored with erythrosine (the composition is discussed in the section "Samples"). Figure 6 (blue (3) and black (4) lines) shows results of the fluorescence measurements with the white tablet (integration time 1 s, 10 replicate measurements were averaged) performed with the Nd:YAG laser (λ_{ex}=266 nm) and with an LED emitting at higher wavelengths (λ_{ex}=360–370 nm) as excitation sources. The fluorescence signal of the analyte using the LED for excitation is shifted to higher wavelengths compared with use of the laser, as expected. Comparing the fluorescence spectra obtained from the white and red tablets (Fig. 6, green (2) and black (4) lines) using the laser as excitation source, the area of the fluorescence signal related to the analyte varies only slightly for the tablets. Only in the wavelength range between 420 and 550 nm is the fluorescence intensity of the spectrum of the red tablet lower than that of the white tablet. This is presumably caused by absorption of the fluorescence by the colorant. A signal of low intensity only (maximum at 570 nm), that can be assigned to the colorant, is detected by using the laser as excitation source (Fig. 6, green line (2)). In contrast, in the fluorescence spectrum using the LED as excitation source, an intense signal of the colorant with a maximum at 600 nm can be observed (Fig. 6, red line (1)).

Overall, the LED provides more information about the colorant, but the laser enables better quantification of the API quinine. Use of different light sources thus enables broad applicability of the setup. In the forensic sciences, determination of intensity ratios of several compounds present in one sample might provide additional information enabling discrimination between an original sample and its counterfeits.

Setup of the design of experiments

We investigated the effect of different physical and chemical conditions on the fluorescence spectra, using the UV laser for excitation. On the basis of the design of experiments, a set of tablets was produced with large-scale commercial equipment including samples of different composition (concentration of active agent and matrix substances), physical properties (hardness), and homogeneity (realized by use of different blending procedures: manual mixing and mixing with commercial equipment).

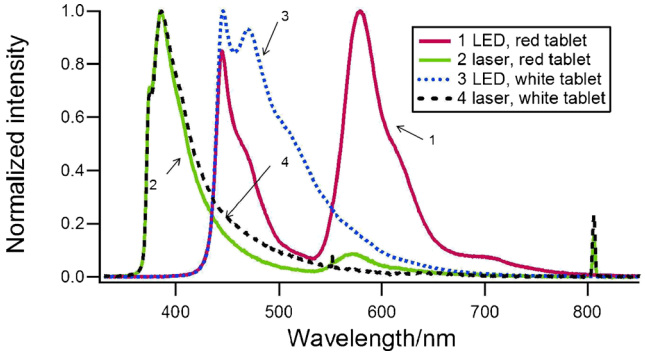

Fig. 6 Fluorescence spectra obtained from colored (red) and uncolored (white) tablets by use of a laser (λ_{ex}=266 nm) and an LED (λ_{ex}=360–370 nm) as excitation source, integration time 1 s (10 replicate measurements were averaged)

Compaction

In the first step, we investigated the effect of the tablet's hardness on fluorescence spectra, which may obscure the chemical information in a fluorescence spectrum (e.g. the amount of the active agent) and therefore complicates data evaluation [14]. We here investigate the applicability of a preprocessing tool (MSC) that has already widely been used in NIR and Raman-spectroscopic applications to remove interferences in spectra related to variations in the physical properties of the sample.

Granulation

Measurements were performed with tablets compressed from raw material of different granulation grain size (average grain sizes 286.8 and 674.0 μm). The effect of grain size on fluorescence spectra was investigated.

Homogeneity

For coarse mixing procedures, for example the manual procedure, distribution of an API in the uncompressed material varies substantially. The aliquots taken for tableting might be homogeneous themselves, but different tablets vary in their API content (inter-tablet homogeneity). In contrast, relatively good mixing will give rise to tablets with a very similar API content, but small variation in the spatial distribution of the API among tablets might remain (intra-tablet homogeneity). For investigation of intra-tablet inhomogeneity, 2D methods based on matrix assisted laser desorption ionization (MALDI) imaging [27] and 2D NIR [28, 29] or Raman [30] spectroscopy are described in the literature. These 2D methods are time-consuming but provide in-depth information about the homogeneity of the sample and information about the spatial distribution of trace contaminants. Inhomogeneity of pharmaceutical dosage forms is also extremely important in the forensic sciences, because they might indicate drugs are counterfeit [31], because of the limited production and/or processing capabilities of illegal laboratories.

We found one study only describing analysis of tablets to determine intra-tablet homogeneity by use of 1D measurements: Vredenbregt et al. [32] reported an NIR method enabling identification of inhomogeneous samples by comparison of spectra obtained from measurements conducted at the tablet's top and bottom. We did not find any study describing investigation of the homogeneity of tablets by use of fluorescence spectroscopy. One study reported in the literature [33] described the use of LIF spectroscopy to investigate the homogeneity of pharmaceutical powders during the blending process. An argon-ion laser at 488 nm was used for excitation, and spectra were recorded during the blending process. The fluorescence signal remained constant as soon as the blending process was completed and the content was homogeneously mixed.

Chemical information

In addition to the ability to discriminate among tablets on the basis of their physical properties, discrimination among tablets containing different amounts of API is essential, because many counterfeit drugs differ in absolute amount of the API compared with the original [9]. The potential to discriminate these by use of fluorescence spectroscopy was described in the sections above. Tablets containing different amounts of API and of different hardness were then investigated.

Having discussed, in detail, the effect of separate properties in the sections below, we then proceed investigating possible discrimination among tablets differing in all these properties (in the section "Combined effects of all properties" below).

All spectra were recorded in the wavelength range between 175 and 994 nm. Data were subjected to PCA with and without preprocessing (MSC, only in the range between 270 and 740 nm because this range covers the full emission range of the analytes quinine sulfate dihydrate and caffeine). The distance between the surface of the sample and the end of the fiber was set to 1.3 cm for all measurements.

Discrimination of tablets with different chemical and physical properties

The effect of the tablet's hardness on fluorescence spectra

Measurements performed with Samples L1–L4 (manufactured with different compression force but the same composition) yielded spectra with an overall trend of increasing fluorescence intensity for tablets manufactured with lower compression force (Fig. 7a), thus allowing their discrimination. However, the intensity of the fluorescence emission for the Samples L1 and L2 (manufactured with optimum and high compression force) is approximately identical.

The higher fluorescence intensity of spectra of tablets manufactured under low compression force (L1, 2 vs. L3, 4) might be caused by:

1. greater roughness of the sample's surface and thus more molecules on the surface available for interaction with the excitation beam; and
2. greater reflectance and/or scattering of the excitation beam on the surface of the sample as a result of its greater compactness.

MSC, widely used to remove effects in spectra related to the sample's physical properties, was applied to the dataset (Fig. 7c). Preprocessed spectra are indistinguishable (Fig. 7c) even when such mathematical techniques as PCA are used (Fig. 7d), demonstrating that variations between the spectra are solely related to scattering effects.

Subjecting the raw-data to PCA enables discrimination of tablets on the basis of hardness by use of PC-1, which explains nearly 100 % of the variance (with 14 000 units for the maximum difference between the lowest and highest scores for spectra of tablets of different hardness). Small-scale variations (only 500 units) for scores on PC-1 for the preprocessed data can be attributed to statistical effects.

Similar results have been reported for other methods. Morisseau et al. [34] observed an increase of NIR absorbance with increasing sample hardness, explainable by less diffuse reflectance because of the smoother surface. Similar results were obtained by Blanco et al. [35], also by use of NIR spectroscopy.

Granulation and grain size

Tablets manufactured with different hardness and different grain sizes (L and K) can be distinguished by PCA on the basis of the raw spectra (Fig. 8a): Scores on PC-1 explain almost 100 % of the variance between spectra from tablets varying in hardness (different symbols in Fig. 8a). However, spectra of samples manufactured with the same compression force but different granule grain size vary on a small scale only within the score values on PC-2 (Fig. 8a, same symbol but different color and filling). The score values on PC-2 for Series K with grains of large diameter are negative; Series L, manufactured with material of smaller grain size, have positive score values on PC-2. Only a small amount of the spectral difference is explained by this principle component (close to 0 % of the variance). Applying MSC to the dataset removes the differences in the spectra caused by the sample's physical properties. Discrimination based on granule grain size is now possible via the score values on PC-1 explaining 82 % of the variance. Variations in the spectra of the tablets of the Series L and K are, presumably, caused by quenching effects or the

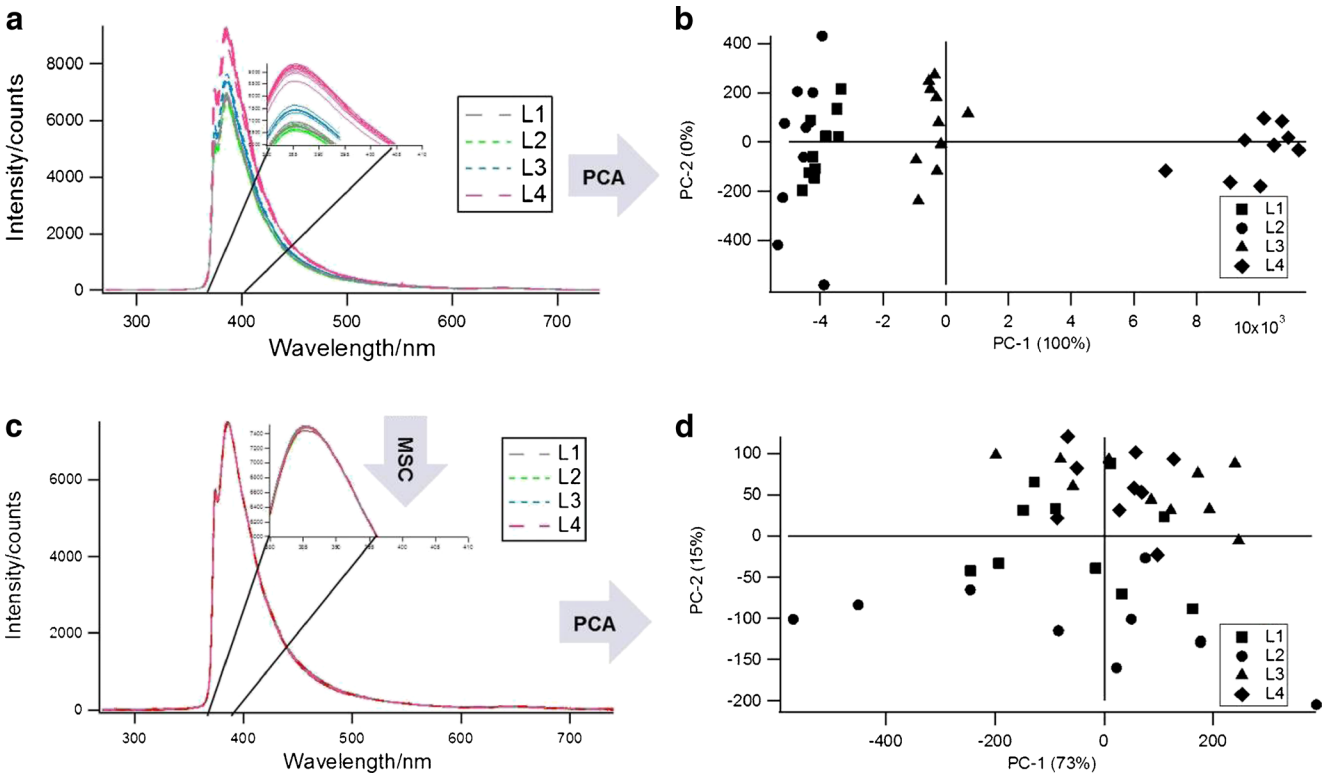

Fig. 7 Fluorescence spectra of tablets compressed with four different compression forces (Series L, numbers: 1=19.6 kN, 2=13.8–14.0 kN, 3=8.5–8.6 kN, 4=5.7–5.8 kN) without (**a**) and with (**c**) data-preprocessing; data were subjected to PCA (mean centered data, score plots PC-2 vs. PC-1) without (**b**) and with (**d**) data-preprocessing by use of the MSC algorithm; λ_{ex}=266 nm

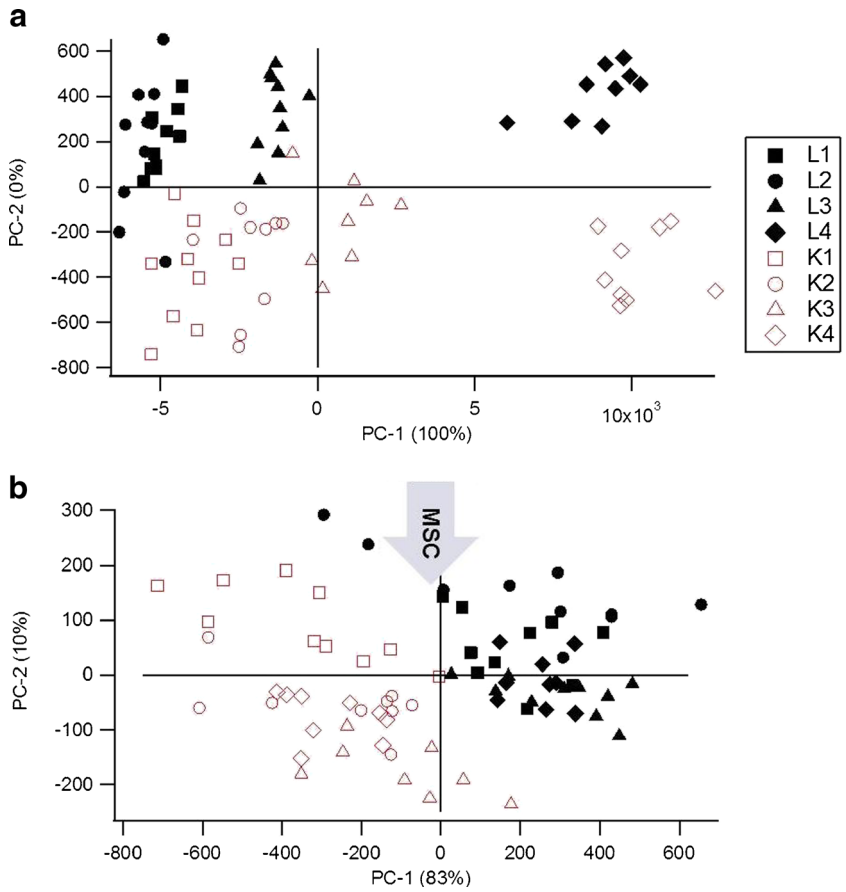

Fig. 8 Score plots of PCA (PC-2 vs. PC-1, mean centered spectra) without (**a**) and with (**b**) data preprocessing (MSC), Samples: L (*filled symbols*), K (*unfilled symbols*); numbers: 1=19.6 kN, 2=13.8–14.0 kN, 3=8.5–8.6 kN, 4=5.7–5.8 kN; grain size L: average grain size=286.8 μm, K: average grain size=674.0 μm; no differences in the chemical composition; λ_{ex}=266 nm

different microenvironments of the samples. Spectra of tablets in Series L are represented by negative scores, Spectra of tablets in Series K by positive scores. However, the absolute difference in score values is small. Therefore granule grain size does not need to be taken into account when investigating qualitative and quantitative aspects of a tablet. Comparable data from other studies are not known to us.

Homogeneity

The potential of the method to discriminate homogeneously mixed from inhomogeneously mixed tablets via the corresponding fluorescence spectra was investigated by using Series L (homogeneous samples) and m (inhomogeneous samples). We assume subsampling effects to be negligible for the measurements presented in this section, because the intensity maxima in the spectra differed only slightly ($RSD_{max,m1}$= 4.6 %, n=10; $RSD_{max,L1}$=1.4 %, n=10) as is expected even for differences in homogeneity, because a large area on the sample was probed. The higher RSD value for the intensity maxima in the spectra recorded for the inhomogeneous samples is already an indication of sample inhomogeneity. Subjecting the raw dataset to a PCA (Fig. 9a) yielded clusters in the score plot (PC-2 vs. PC-1) representing tablets of the same hardness (Series L and m, Table 2) and homogeneity (homogeneous samples, filled symbols; inhomogeneous samples, unfilled symbols). Spectra of tablets varying in hardness can be distinguished via PC-1, except for L1 and L2, because the corresponding clusters overlap. Spectra of the inhomogeneous tablets (Series m) can be distinguished by different score values on PC-1 (99 % of the variance of the dataset) and PC-2. Negative values on PC-1 are correlated with high compression force (used to compress the material) but also homogeneity. Scores on PC-2 only explain 1 % of the variance of the dataset. Negative score values on PC-2 are correlated with homogeneity and low compression force (used to manufacture the tablets).

To prove that variations in the dataset are not related to the physical properties of the sample but are caused by a different chemical composition within the probed area, because of variations in homogeneity, spectra were preprocessed using the MSC algorithm. We assume MSC to be an appropriate tool for data preprocessing, because our results presented in the section "Sensitivity and linearity" show that the fluorescence intensity depends linearly on concentration within the small "concentration range" investigated (on the surface of the samples because of variations in the mixing procedure). As shown in the section "The effect of the tablet's hardness on fluorescence spectra", MSC removes interferences in spectra related to the physical properties of a sample; only information

related to the chemical information of the spectra is left. Inhomogeneous mixing causes variations with regard to the distribution of the fluorophore in the sample. Discrimination of tablets varying in homogeneity by use of PCA is therefore possible for MSC-preprocessed spectra (Fig. 9b). Samples can now be classified into two groups on the basis of their fluorescence spectra: homogeneous tablets and inhomogeneous tablets can be distinguished on the basis of on their scores on PC-1. Ninety percent of the variance in the spectra can be explained via PC-1 with a clear indication of positive PC-1 scores being correlated with inhomogeneity. Higher variation within the clusters related to inhomogeneous tablets is caused by the random distribution of the active agent on the surface of the tablets (compare RSD values above). Within the group of spectra of inhomogeneously mixed samples, slight grouping related to the tablet's hardness can still be observed after preprocessing by use of the MSC algorithm (see also discussion on loadings, in the section "Combined effects of all properties").

Chemical composition

Samples of different composition (Series L, N), but also varying in hardness (Numbers 1–4) were investigated. The MSC-preprocessed dataset was subjected to PCA. Two clusters were obtained in the PCA score plot (Fig. 10), as expected for spectra of tablets of two different compositions (L, 1 % (*w*/*w*); N, 4 % (*w*/*w*) quinine sulfate). The score values on PC-1 vary from 7000 to 12 000 units for the two clusters. For spectra of tablets of Series L the scores on PC-2 vary slightly (800 units), explaining 4 % of the variance of the dataset. In contrast, for spectra of tablets of Series N some clustering related to the hardness of the tablet over 5000 units is observed on PC-1 and some variation in the score values is observed on PC-2. This can be ascribed to the manufacturing process: tablets of Series N were manufactured by direct compression, those of Series L with a granulation step before compression. Use of different manufacturing processes can be assumed to affect the structure of the tablets, causing scattering by the tablet's surface, and (but to a lesser extent) the chemical microenvironment of the active agent, causing clustering in the score plot.

Discrimination of tablets containing different amounts of the API by use of their spectra has been demonstrated for other methods, for example Raman or NIR. For example, Vredenbregt et al. [32] reported a method in which clustering in the score plot of spectra was observed for tablets containing different amounts of API. Tablets containing 50 and 100 mg sildenafil citrate could hardly be discriminated via the score values on PC-1, but these tablets could be distinguished well from tablets containing less of the active agent (25 mg).

Combined effects of all properties

The suitability of the setup for discrimination among tablets differing in one or two properties by means of the corresponding fluorescence spectra has already been discussed in previous sections. To investigate the potential of the method for the set of tablets of the full DoE, spectra of tablets of Series L, m, N, and K, including variations with regard to homogeneity (m vs. L), grain size (L vs. K), chemical composition (N vs. L), and hardness (Numbers 1–4) were subjected to PCA, initially without MSC preprocessing (Fig. 11a). Of course, most aspects of the previous section are again visible, but the PCA of the whole DoE clearly shows the discriminating power of solid-state fluorescence of tablets varying in multiple conditions (physical and chemical).

The score plot contains one large cluster with high score values on PC-1 and negative score values on PC-2 comprising the full Series N containing 4 % of the fluorophore (instead of 1 % for all other tablets). This cluster is quite disperse because of sample properties caused by the direct tableting process (also discussed in the section "Chemical composition"). Clusters of score values representing Series L and K are hardly separated, which was expected on the basis of our results in the section "Granulation and grain size". There is a clear trend for score values representing Series L, K, and m, which are clearly arranged along two parallel lines in the score plot: PC-1 is clearly related to variations in the spectra caused by differences in the hardness of the tablets. Overall, without preprocessing, PC-2 is related to the chemical composition (homogeneity) or microenvironment and the tableting process (direct vs. granulation).

The loadings plot shown in Fig. 12a (PC-2 vs. PC-1) clearly shows that the wavelengths close to the maximum of a fluorescence spectrum have a strong effect on the model (wavelength range 380–390 nm). The maximum intensity is strongly affected by physical properties, e.g. the hardness of the tablet, in accordance with the results presented in the section "The effect of the tablet's hardness on fluorescence spectra" and thus strongly determines PC-1. The intensity in the wavelength range 465–475 nm has a strong effect on the scores on PC-2 and can be assigned to the composition of the sample. This means that without data preprocessing by use of MSC, tablets can mostly be characterized with regard to their physical properties. This enables assessment of the quality of the manufacturing process.

To stress the chemical information, which is only represented by PC-2 explaining 13 % of the variance, spectra were preprocessed by applying MSC. Now, three classes of tablets can easily be distinguished via scores on PC-1 (explaining 96 % of the total variance). PC-1 score values now mostly reflect chemical information about the sample but also some aspects of the manufacturing process (L/K vs. m series): With an increasing amount of API, higher PC-1-scores are obtained

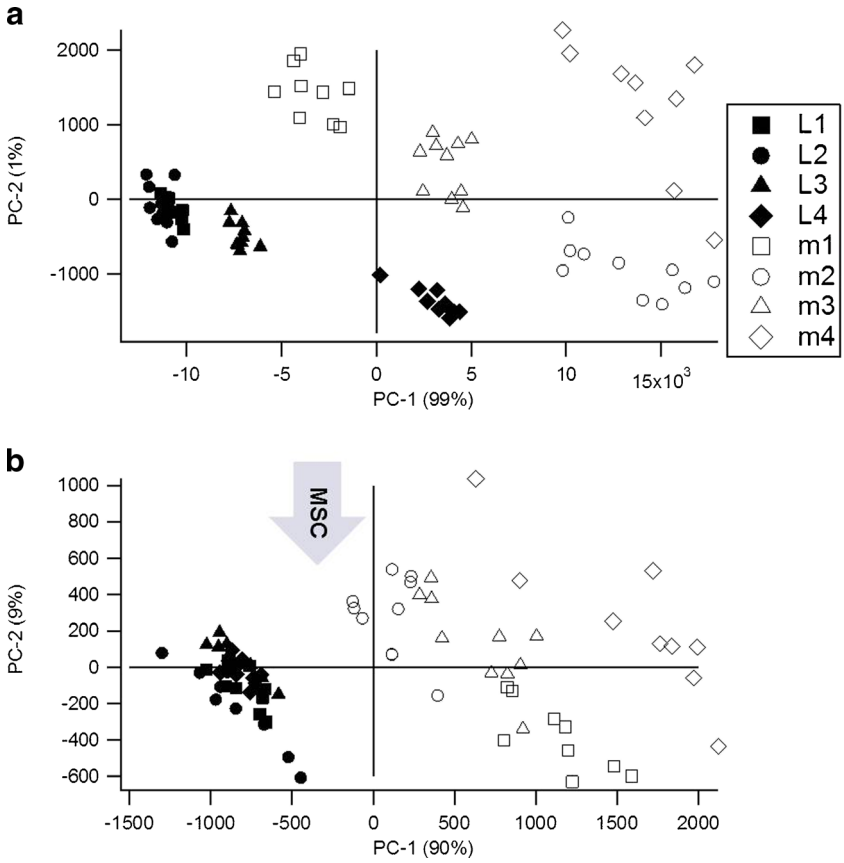

Fig. 9 Score plots of PCA (mean centered data, PC-2 vs. PC-1) with (**b**) and without (**a**) data preprocessing by use of MSC; samples: m (inhomogeneous samples, *unfilled symbols*), L (homogeneous samples, *filled symbols*); numbers: 1=19.6 kN, 2=13.8–14.0 kN, 3=8.5–8.6 kN, 4=5.7–5.8 kN; same chemical composition; λ_{ex}=266 nm

(Fig. 11b). Clearly, with only 4 % of variance explained by scores on PC-2, scattering effects as a result of the different physical properties of the sample were removed by MSC; now the chemical information in the data is stressed. Further subclustering is dominated by the tableting process (L/K vs. m series) and the chemical microenvironment induced by the compaction pressure, but to a much smaller extent than for the results from the raw data. For Series N, especially, subclustering is still clearly visible in Fig. 11b (PC-2 score-range between −3000 and +3000). Clusters representing the spectra of tablets with different grain size (K and L) strongly overlap (lower scores on PC-1), but both series of tablets are well distinguishable from the inhomogeneous samples (m, black, unfilled symbols).

Figure 12b shows the corresponding loadings plot (MSC-preprocessed data). It confirms that the preprocessing significantly reduces the effect of the maximum intensity in the wavelength range between 370 and 384 nm on clustering on PC-1. This wavelength range, strongly affected by the physical properties of the tablet (hardness and manufacturing process), is now strongly correlated with PC-2. Clustering of score values on PC-1 can be assigned to a different composition of the corresponding sample causing spectral variations in the wavelength range between 460 and 470 nm. In

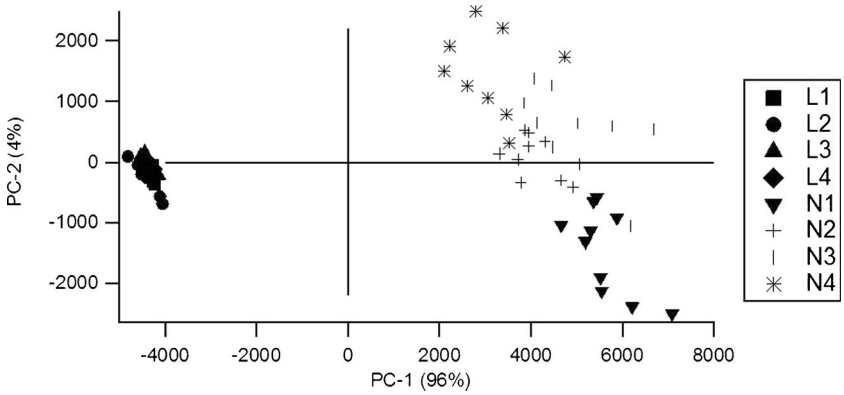

Fig. 10 Score plot of a PCA (PC-2 vs. PC-1, preprocessed, mean centered data; samples: L (1 % (*w*/*w*) quinine sulfate dihydrate), N (4 % (*w*/*w*) quinine sulfate dihydrate); numbers: 1=19.6 kN, 2=13.8–14.0 kN, 3=8.5–8.6 kN, 4=5.7–5.8 kN); λ_{ex}=266 nm

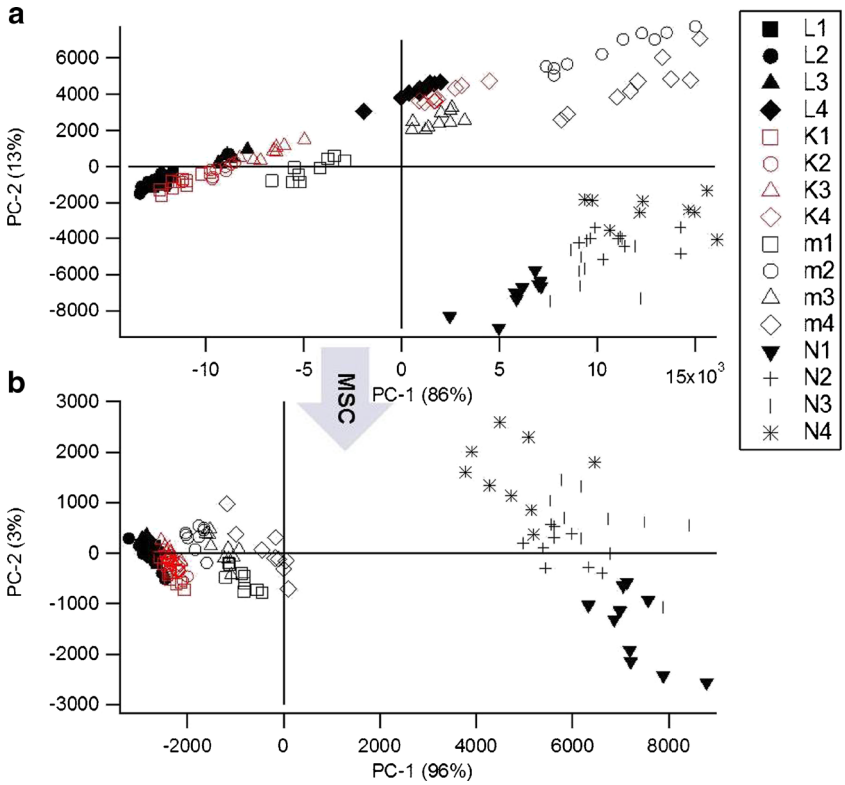

Fig. 11 PCA overview (mean centered data): score-plot PC-2 vs. PC-1 before (**a**) and after (**b**) data preprocessing by use of the MSC-algorithm; samples: Series L, N, m, K; λ_{ex}=266 nm; series description is given in Tables 2 and 3

comparison with the result of the PCA before preprocessing, the wavelengths relevant to clustering changed: the maximum intensity in the wavelength range between 380 and 390 nm is strongly affected by scattering effects and causes clustering on PC-1. After applying MSC, changes in spectra because of the tablet's hardness now cause hardly any clustering of PC-1 scores (loading values close to zero), showing that differences in scattering effects have been removed by MSC. Changes in the chemical microenvironment as a result of compression force and manufacturing process are, however, still visible in PC-2 and in the wavelength range of the maximum intensity. Overall, with MSC, information related to chemical composition is stressed: a high concentration of API is correlated with positive scores on PC-1.

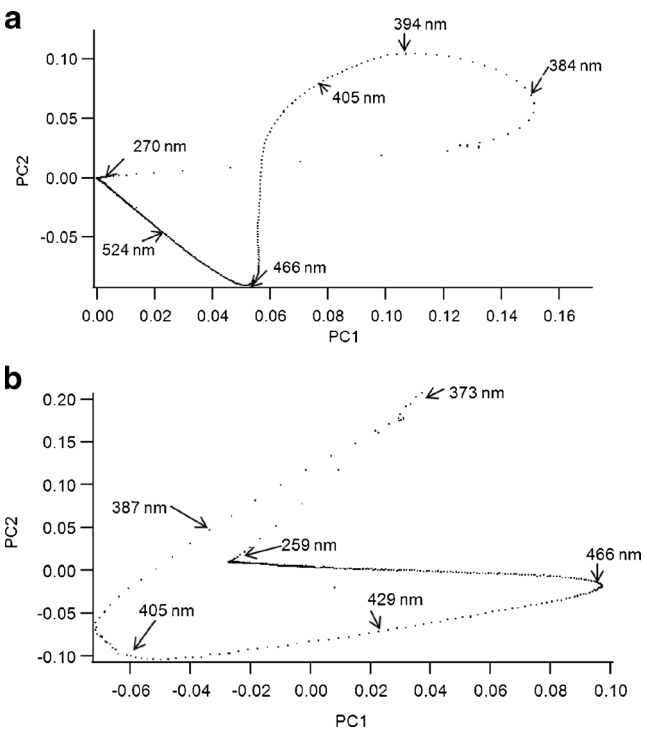

Fig. 12 Loadings plot of the PCA (dataset: spectra of Series L, K, m, N) PC-2 vs. PC-1 (**a**) without preprocessing and (**b**) with preprocessing (MSC).

Conclusion

The setup presented in this paper provides a powerful technique for analysis of pharmaceutical solids by laser-induced fluorescence spectroscopy; repeatability is high and the technique requires no sample preparation. The distance between the end of the optical fiber and the sample's surface can easily be optimized because of the use of a y-fiber mounted in reflectance geometry that is easy to handle. Use of a UV-laser (λ_{ex}=266 nm) as an excitation source provides broad applicability for many natively fluorescent analytes. The number of fluorophores that can be analyzed with this setup can be increased changing the light source, as was demonstrated for LED vs. laser excitation for colored tablets. Integration of our

system into a solid detector head will further increase the system's robustness. Regarding analysis of pharmaceutical solids in the forensic sciences and process analysis, we show here that fluorescence spectroscopy can provide additional information to Raman or NIR methods, especially with regard to determination of trace compounds or the chemical microenvironment of the active agent. Our setup enables detection of trace compounds down to a concentration of 0.01 % (*w*/*w*) for ASA, 1 % (*w*/*w*) for quinine sulfate dihydrate, and 1 % (*w*/*w*) for chloroquine diphosphate. However, it also has disadvantages, for example re-absorption, for analytes with small Stokes-shifts, and the destructive nature of laser irradiation. By using a large DoE for tablets differing in both chemical and physical properties, we were able to demonstrate the discriminative power of the setup for tablets varying in hardness, chemical composition, and homogeneity. The setup is robust with regard to variations in the grain size of the granules used in the manufacturing process. Using both raw and MSC-preprocessed data, information about both physical quality and composition can be obtained from fluorescence spectra.

The instrumental setup used in this study was developed as part of a project funded by the German Federal Ministry of Education and Research (BMBF). It will be combined with other spectroscopic techniques (Raman, NIR, UV–visible) in a multi-detector head benefiting from the advantages of each individual technique, for example the high sensitivity of fluorescence spectroscopy and the penetration depth of Raman spectroscopy. We did not find a comparable study in literature investigating such a broad variety of properties.

Acknowledgements We thank Jennifer Oppenberg (University of Münster, Germany) for her introduction to the fabrication of tablets. The help of Dr Jan Pöggeler (Forschungszentrum Jülich, Germany) is gratefully acknowledged. This project was partially funded by the Federal Ministry of Education and Research (BMBF), FZK: 13 N12012. This work was partially funded by the Excellence Initiative, a jointly funded program of the German federal and state governments, organized by the German Research Foundation (DFG).

References

1. Aaltonen J, Gordon KC, Strachan CJ, Rades T (2008) Perspectives in the use of spectroscopy to characterise pharmaceutical solids. Int J Pharm 364(2):159–169
2. Jivraj M, Martini LG, Thomson CM (2000) An overview of the different excipients useful for the direct compression of tablets. Pharmaceut Sci Tech Today 3(2):58–63
3. Boukouvala F, Niotis V, Ramachandran R, Muzzio FJ, Ierapetritou MG (2012) An integrated approach for dynamic flowsheet modeling and sensitivity analysis of a continuous tablet manufacturing process. Comput Chem Eng 42(0):30–47
4. Abu Bakar NF, Mujumdar A, Urabe S, Takano K, Nishii K, Horio M (2007) Improvement of sticking tendency of granules during tabletting process by pressure swing granulation. Powder Technol 176(2–3):137–147
5. Zarie ES, Kaidas V, Gedamu D, Mishra YK, Adelung R, Furkert FH, Scherließ R, Steckel H, Groessner-Schreiber B (2012) Solvent free fabrication of micro and nanostructured drug coatings by thermal evaporation for controlled release and increased effects. PLoS One 7(8):e40746
6. Rodionova OY, Houmøller LP, Pomerantsev AL, Geladi P, Burger J, Dorofeyev VL, Arzamastsev AP (2005) NIR spectrometry for counterfeit drug detection: A feasibility study. Anal Chim Acta 549(1–2):151–158
7. Dégardin K, Roggo Y, Been F, Margot P (2011) Detection and chemical profiling of medicine counterfeits by Raman spectroscopy and chemometrics. Anal Chim Acta 705(1):334–341
8. Been F, Roggo Y, Degardin K, Esseiva P, Margot P (2011) Profiling of counterfeit medicines by vibrational spectroscopy. Forensic Sci Int 211(1–3):83–100
9. Holzgrabe U (2009) Problem Arzneimittelfälschungen in Afrika und Südostasien. Gefälschte Antimalariamittel und mehr. Pharm Unserer Zeit 38(6):560–562
10. Mizobe Y, Hinoue T, Yamamoto A, Hisaki I, Miyata M, Hasegawa Y, Tohnai N (2009) Systematic Investigation of Molecular Arrangements and Solid-State Fluorescence Properties on Salts of Anthracene-2, 6-disulfonic Acid with Aliphatic Primary Amines. Chem-A Eur J 15(33):8175–8184
11. Wehry EL (1997) Molecular fluorescence and phosphorescence spectrometry. In: Settle F (ed) Handbook of instrumental techniques for analytical chemistry, 1st. edn. Prentice Hall, Upper Saddle River
12. Navalón A, Blanc R, del Olmo M, Vilchez JL (1999) Simultaneous determination of naproxen, salicylic acid and acetylsalicylic acid by spectrofluorimetry using partial least-squares (PLS) multivariate calibration. Talanta 48(2):469–475
13. Moreira AB, Dias ILT, Neto GO, Zagatto EAG, Kubota LT (2004) Solid-phase fluorescence spectroscopy for the determination of acetylsalicylic acid in powdered pharmaceutical samples. Anal Chim Acta 523(1):49–52
14. Martens H, Nielsen JP, Engelsen SB (2003) Light Scattering and Light Absorbance Separated by Extended Multiplicative Signal Correction. Application to Near-Infrared Transmission Analysis of Powder Mixtures. Anal Chem 75(3):394–404
15. Kessler W (2007) Multivariate Datenanalyse für die Pharma-, Bio- und Prozessanalytik. Wiley-VCH, Weinheim
16. Heraud P, Wood BR, Beardall J, McNaughton D (2006) Effects of pre-processing of Raman spectra on in vivo classification of nutrient status of microalgal cells. J Chemom 20(5):193–197
17. Roggo Y, Chalus P, Maurer L, Lema-Martinez C, Edmond A, Jent N (2007) A review of near infrared spectroscopy and chemometrics in pharmaceutical technologies. J Pharm Biomed Anal 44(3):683–700
18. Song L, Hennink E, Young IT, Tanke HJ (1995) Photobleaching kinetics of fluorescein in quantitative fluorescence microscopy. Biophys J 68(6):2588–2600
19. Oujja M, Vázquez-Calvo C, Sanz M, Buergo MÁ, Fort R, Castillejo M (2012) Laser-induced fluorescence and FT-Raman spectroscopy for characterizing patinas on stone substrates. Anal Bioanal Chem 402(4):1433–1441
20. Kim M, Chung H, Woo Y, Kemper M (2006) New reliable Raman collection system using the wide area illumination (WAI) scheme combined with the synchronous intensity correction standard for the analysis of pharmaceutical tablets. Anal Chim Acta 579(2):209–216
21. Villari A, Micali N, Fresta M, Puglisi G (1992) Simultaneous spectrophotometric determination in solid phase of aspirin and its impurity salicylic acid in pharmaceutical formulations. J Pharm Sci 81(9):895–898
22. Head W (1961) Investigation of the applicability of solid state fluorescence to pharmaceutical analysis. J Pharm Sci 50(12):1041–1044
23. Edwards L (1950) The hydrolysis of aspirin. A determination of the thermodynamic dissociation constant and a study of the reaction

kinetics by ultra-violet spectrophotometry. Trans Faraday Soc 46: 723–735
24. Milofsky R, Bauer E (1997) Capillary electrophoresis with post-column addition of terbium and sensitized lanthanide-ion luminescence detection for the determination of diflunisal and salicylic acid. J High Resolut Chromatogr 20(12):638–642
25. Chen RF (1967) Some characteristics of the fluorescence of quinine. Anal Biochem 19(2):374–387
26. Merckle P, Kovar K-A (1998) Assay of effervescent tablets by near-infrared spectroscopy in transmittance and reflectance mode: acetylsalicylic acid in mono and combination formulations. J Pharm Biomed Anal 17(3):365–374
27. Earnshaw CJ, Carolan VA, Richards DS, Clench MR (2010) Direct analysis of pharmaceutical tablet formulations using matrix-assisted laser desorption/ionisation mass spectrometry imaging. Rapid Commun Mass Spectrom 24(11):1665–1672
28. Sasic S, Kong A, Kaul G (2013) Determining API domain sizes in pharmaceutical tablets and blends upon varying milling conditions by near-infrared chemical imaging. Anal Methods 5(9):2360–2368
29. Cruz J, Blanco M (2011) Content uniformity studies in tablets by NIR-CI. J Pharm Biomed Anal 56(2):408–412
30. Nakamoto K, Urasaki T, Hondo S, Murahashi N, Yonemochi E, Terada K (2013) Evaluation of the crystalline and amorphous states of drug products by nanothermal analysis and Raman imaging. J Pharm Biomed Anal 75:105–111
31. Puchert T, Lochmann D, Menezes JC, Reich G (2010) Near-infrared chemical imaging (NIR-CI) for counterfeit drug identification—A four-stage concept with a novel approach of data processing (Linear Image Signature). J Pharm Biomed Anal 51(1):138–145
32. Vredenbregt MJ, Blok-Tip L, Hoogerbrugge R, Barends DM, Dd K (2006) Screening suspected counterfeit Viagra® and imitations of Viagra® with near-infrared spectroscopy. J Pharm Biomed Anal 40(4):840–849
33. Lai C-K, Holt D, Leung JC, Cooney CL, Raju GK, Hansen P (2001) Real time and noninvasive monitoring of dry powder blend homogeneity. AlChE J 47(11):2618–2622
34. Morisseau K, Rhodes C (1997) Near-Infrared Spectroscopy as a Nondestructive Alternative to Conventional Tablet Hardness Testing. Pharm Res 14(1):108–111
35. Blanco M, Alcalá M, González JM, Torras E (2006) A process analytical technology approach based on near infrared spectroscopy: Tablet hardness, content uniformity, and dissolution test measurements of intact tablets. J Pharm Sci 95(10):2137–2144